The AAPS Journal, Vol. 12, No. 4, December 2010 (© 2010)
DOI: 10.1208/s12248-010-9234-9

Research Article

Pharmacodynamics-Mediated Drug Disposition (PDMDD) and Precursor Pool Lifespan Model for Single Dose of Romiplostim in Healthy Subjects

Yow-Ming C. Wang,[1,3] Wojciech Krzyzanski,[2] Sameer Doshi,[1] Jim J. Xiao,[1] Juan Jose Pérez-Ruixo,[1] and Andrew T. Chow[1]

Received 2 June 2010; accepted 20 September 2010; published online 21 October 2010

Abstract. The objective of this study was to characterize the pharmacokinetics and pharmacodynamics (PK-PD) of romiplostim after single-dose administration in healthy subjects. The mean serum romiplostim concentrations (PK data) and mean platelet counts (PD data) collected from 32 subjects receiving a single intravenous (0.3, 1 and 10 μg/kg) or subcutaneous (0.1, 0.3, 1, and 2 μg/kg) dose were fitted simultaneously to a mechanistic PK-PD model based on pharmacodynamics-mediated drug disposition (PDMDD) and a precursor pool lifespan concept. The two-compartment PK model incorporated receptor-mediated endocytosis and linear mechanisms as parallel elimination pathways. The maximal concentration of receptors (assumed to be proportional to the platelet count), the equilibrium dissociation constant, and the first-order internalization rate constant for endocytosis of the drug-receptor complex were 0.022 fg/platelet, 0.131 ng/mL, and 0.173 h^{-1}, respectively. Romiplostim concentration stimulates the production of platelet precursors via the Hill function, where the SC_{50} was 0.052 ng/mL and S_{max} was 11.2. The estimated precursor cell and platelet lifespans were 5.9 and 10.5 days, respectively. Model-based simulations revealed that the romiplostim exposure and the platelet response are both dependent on the dose administered and the baseline platelet counts. Also, weekly dosing produced a sustained PD response while dosing intervals ≥2 weeks resulted in fluctuating platelet counts. Thus, the mechanistic PK-PD model was suitable for describing the romiplostim PK-PD interplay (PDMDD), the dose-dependent platelet stimulation, and the lifespans of thrombopoietic cell populations.

KEY WORDS: lifespan model; pharmacodynamics-mediated drug disposition (PDMDD); platelets; romiplostim; thrombopoiesis receptor agonist.

INTRODUCTION

Thrombopoietin (TPO), a primary regulator in the megakaryocytic lineage, plays a key role in platelet production. TPO stimulates the proliferation, differentiation, and maturation of platelet precursor cells such as megakaryocytes. Binding of TPO to its receptor, c-Mpl, followed by cellular signal transduction processes including tyrosine phosphorylation of the receptor (1) leads to increased platelet counts. TPO is predominantly produced in the liver by hepatocytes. The bone marrow, kidney, brain, testis, and spleen are organs expressing TPO mRNA (2,3). The free TPO circulating level is inversely related to platelet count (4).

As a variety of disease states influence the levels of endogenous TPO (eTPO), the development of thrombopoietin receptor agonists (TRA) has been undertaken to fulfill the unmet medical needs of patients with a diagnosis of immune thrombocytopenia (ITP), chronic liver disease, AIDS, myelodysplastic syndrome, or in cancer patients undergoing chemotherapy. However, the effort was hampered by the formation of neutralizing antibodies cross-reacting with eTPO in healthy subjects (5,6).

Romiplostim (AMG 531, Nplate®) is a novel TPO mimetic peptibody comprising two human immunoglobulin IgG_1 Fc domains, each of which is covalently linked to a peptide chain containing two TPO receptor-binding peptides (7). Romiplostim has no sequence homology with eTPO, reducing the potential for the development of cross-reacting antibodies (7). Romiplostim activates the TPO receptor to stimulate the growth and maturation of megakaryocytes, with a consequent increase in platelet production (7). *In vitro*, romiplostim binds to human c-Mpl receptors with a dissociation constant value of 0.51 nM, which is lower than the recombinant human TPO (8,9). Dose-dependent increases in platelet counts were observed in several preclinical species and humans. At this time, romiplostim is licensed for the treatment of adult patients with chronic ITP in the USA, EU, Australia, Switzerland, Canada, and Mexico.

Romiplostim single-dose PK data in healthy subjects showed a dose-dependent volume of distribution and clearance,

[1] Pharmacokinetics and Pharmacometrics, Pharmacokinetics and Drug Metabolism Department, Amgen Inc., One Amgen Center Drive, Thousand Oaks, California 91320, USA.
[2] Department of Pharmaceutical Sciences, University at Buffalo, State University of New York, Buffalo, New York, USA.
[3] To whom correspondence should be addressed. (e-mail: yowc@amgen.com)

which decreased with increasing dose (7). Target-mediated disposition is a potential cause for the observed nonlinearity (8,10,11). We developed a mathematical model, based on the concepts of target-mediated drug disposition and precursor pool platelet lifespan, to characterize the pharmacokinetics and pharmacodynamics (PK-PD) of romiplostim using single-dose data, and subsequently used the model to explore the exposure–response relationship following the administration of romiplostim. The romiplostim PK-PD model was further used to assess the contribution of the receptor-mediated drug clearance, and to support the dosing regimen selection for ITP subjects.

METHODS

Study Design

The analysis dataset was derived from a healthy volunteer phase I study, details of which were previously reported (7). Healthy male and female non-obese subjects (body mass index, <30 kg/m^2), aged between 18 and 50 years without risk factors for cardiovascular disease were allowed to participate in the study. Eligible women were either surgically sterilized or postmenopausal. The study was conducted in accordance with principles for human experimentation as defined in the International Conference on Harmonization Good Clinical Practice guidelines and the principles of the Declaration of Helsinki. The study was approved by the corresponding IRB, and informed consent was obtained from each subject

Romiplostim was administered as a single intravenous (IV) dose of 0.3, 1, or 10 μg/kg or subcutaneous (SC) dose of 0.1, 0.3, 1, or 2 μg/kg. There were four romiplostim-treated subjects in each dose group, except for the 2 μg/kg SC group that consisted of eight subjects. Correspondingly, there were 16 placebo-treated subjects, two per group, except the 2 μg/kg SC group.

Venous blood samples were collected before dosing and at 0.083, 0.25, 0.5, 1, 2, 4, 8, and 12 h and then 1, 1.5, 2, 4, 7, 9, 10, 11, 12, 13, 14, 16, and 19 days after dosing for the determination of romiplostim serum concentrations. All blood samples were centrifuged, and separated serum was stored at −70°C until the analysis was conducted. Platelet counts were determined from blood samples collected as part of a complete blood cell count at screening, before dosing, and on study days 2, 3, 5, 8, 10, 11, 12, 13, 14, 15, 17, 20, 28, and 42 using a hematology analyzer.

Bioanalytical Assay

A validated modified colorimetric enzyme-linked immunosorbent assay (ELISA) was used to determine romiplostim serum concentrations. A polyclonal rabbit antibody against the c-Mpl-binding peptide domain of romiplostim was used as both the capture antibody and the detection antibody (7). The assay had a quantification limit of 0.018 ng/mL (range, 0.018–0.500 ng/mL). The inter-assay variability ranged from 3.8% to 14%, and the assay error ranged from 7% to 17%.

Software

A simultaneous PK-PD analysis was performed with NONMEM (version V, level 1.1; GloboMax, Hanover, MD, USA). The model was coded in NONMEM using the ADVAN6 library routine and first-order conditional estimation (FOCE) method was used to estimate the model parameters. The model was executed using the Compaq Visual FORTRAN Compiler version 6.6. S-PLUS (version 6.2; Insightful Corporation, Seattle, WA, USA) was used for all data preparation and graphical displays.

Pharmacokinetic Model

To characterize the time course of romiplostim serum concentrations, a subtype of target-mediated drug disposition (TMDD) model called pharmacodynamics-mediated drug disposition (PDMDD) model (Fig. 1) was used. The subcutaneous absorption of romiplostim was represented with the first-order absorption rate, k_a, and absolute bioavailability (F) was also estimated in simultaneously fitting the data obtained after SC and IV administration. After an IV bolus dose, romiplostim was distributed into the central and peripheral compartments, with volumes of V_c and V_p, respectively. The nonspecific distribution into the peripheral compartment was apparent from the experimental data and was characterized by first-order distribution rate processes represented by k_{pc} and k_{cp}. According to the model, romiplostim binding to free receptors was described by a second-order rate constant, k_{on}. The limited total number of receptors (R_{tot}) was used to describe the nonlinearity in the distribution and elimination process and, was assumed to be directly proportional to the platelet count (PLT):

$$R_{tot}=\xi \cdot \mathrm{PLT} \tag{1}$$

where ξ is the proportionality constant that represents the theoretical amount of the c-Mpl receptor per platelet in romiplostim weight equivalent. Although romiplostim has four binding sites to the c-Mpl receptor, given the steric hindrance, the PK model assumed 1:1 stoichiometry to characterize the interaction between romiplostim and the c-Mpl receptor. The drug-receptor complex (DR) formed was dissociated according to a first-order rate constant, k_{off}, and generated free drug and receptor, or was internalized into the cell according to a first-order rate constant, k_{int}. The free romiplostim was also eliminated from the central compartment by a linear pathway quantified by the elimination rate, k_{el}. The differential equations used to describe the amount of free and bound romiplostim are as follow:

$$\frac{\mathrm{d}A_{SC}}{\mathrm{d}t} = -k_a \cdot A_{SC} \tag{2}$$

$$\frac{dA_c}{dt} = k_a \cdot A_{SC} - (k_{el} + k_{cp} + \frac{k_{on}}{V_c} \cdot (\xi \cdot PLT - DR)) \cdot A_c + k_{pc} \cdot A_p + k_{off} \cdot DR \tag{3}$$

$$\frac{dA_p}{dt} = k_{cp} \cdot A_c - k_{pc} \cdot A_p \tag{4}$$

$$\frac{dDR}{dt} = \frac{k_{on}}{V_c} \cdot (\xi \cdot PLT - DR) \cdot A_c - k_{off} \cdot DR - k_{int} \cdot DR \tag{5}$$

where A_c and A_p refer to the amount of free romiplostim in serum and in the peripheral compartment, and the free serum

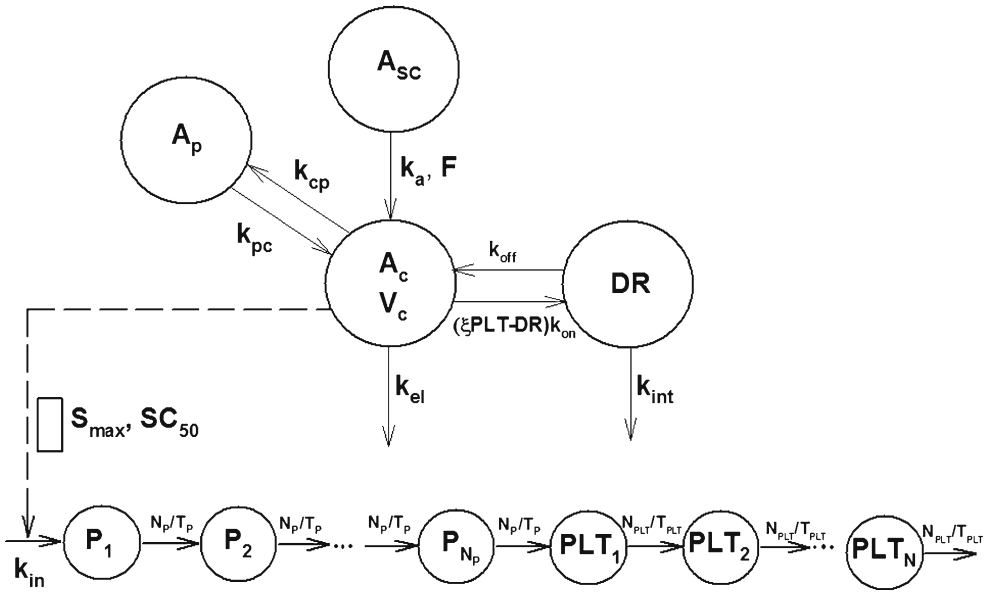

Fig. 1. A PDMDD and lifespan PK/PD model for romiplostim. A_1, A_2, A_3 are the depot, central, and peripheral compartments, respectively. The inter-compartmental transfer rate constants from central to peripheral compartment and from peripheral to central compartment are k_{cp} and k_{pc}, respectively. Drug from the central compartment can be eliminated by a first-order process with a rate constant k_{el}, or can bind to c-Mpl receptors at a rate characterized by k_{on} to form a drug-receptor complex (*DR*), i.e., the DR compartment. This complex may either dissociate (k_{off}) or be internalized and degraded (k_{int}). ξPLT-DR stands for the amount of receptors not bound to drug. ξ is the TPO receptor density/platelet. T_P and T_{PLT} stand for the lifespan of precursor cells and platelets. N_P and N_{PLT} stand for the number of age-compartments for the precursor cells and platelets; N_P=N_{PLT}=10. P_1, P_2, … P_{Np} are the age-compartments for various stages of the precursor cells. PLT_1, PLT_2, … PLT_N are the age-compartments for various stages of the platelets. The sum of platelet counts in all PLT_N compartments is PLT. k_{in} is the rate of production of the precursor cells. S_{max} represents the maximum extent of stimulation and SC_{50} is the concentration required for 50% maximum stimulation. The subcutaneous absorption rate constant is k_a, and F is the absolute bioavailability

concentration C was set equal to A_c/V_c. A_{SC} denotes the amount of romiplostim in the subcutaneous site. To avoid the estimation of the binding constants k_{on} and k_{off}, a quasi-equilibrium assumption between romiplostim and c-Mpl receptors was used (12). The c-Mpl receptor-binding affinity was estimated as the dissociation equilibrium constant (K_D), which was defined as k_{off}/k_{on}. The total amount of drug (A_{tot}) in serum was introduced as the sum of A_c and DR and the diferential equation was as follows:

$$\frac{dA_{tot}}{dt} = k_a \cdot A_{SC} - (k_{el} + k_{cp}) \cdot C \cdot V_c + k_{pc} \cdot A_p - k_{int} \cdot DR \quad (6)$$

The free romiplostim serum concentration was calculated from the quasi-equilibrium equation as follows:

$$C = 0.5 \cdot \left(\frac{A_{tot}}{V_c} - R_{tot} - K_D + \sqrt{\left(\frac{A_{tot}}{V_c} - R_{tot} - K_D\right)^2 + 4 \cdot K_D \cdot \frac{A_{tot}}{V_c}} \right) \quad (7)$$

and the drug-receptor complex was calculated as follows:

$$DR = \frac{R_{tot} \cdot C}{K_D + C} \quad (8)$$

The initial conditions for Eqs. 2, 4, and 6 were set as:

$$A_{sc}(0) = F \cdot Dose_{SC},\ A_p(0) = 0,\ \text{and}\ A_{tot} = Dose_{IV} \quad (9)$$

Pharmacodynamic Model

To quantify the increases in production of platelets resulting from romiplostim administration, the concept of maturation-structured cytokinetic model introduced previously by Harker *et al.* (13) and later used by Roskos *et al.* (14) and Perez-Ruixo *et al.* (15) was applied. The model accounted for the development and maturation of platelet precursors in the bone marrow and the release and aging of platelets in blood. The backbone structure of such a model is a series of compartments linked in a catenary fashion by first-order cell transfer rates. A cascade of N_P=10 age compartments with the transfer rate constants equal to N_P/T_P were selected to account for development and maturation of megakaryocyte cells, where T_P is the mean lifespan of these precursor cells. Similarly, a cascade of N_{PLT}=10 age compartments represented the circulating platelets and the first-order rate constant between the aging compartments was N_{PLT}/T_{PLT}, where T_{PLT} is the mean lifespan of these platelets. As the precursor cells and the platelets progressed through the series of age compartments, their mean ages increased by $T_P/$

Table I. A Summary of Romiplostim PK-PD Parameter Estimates

Parameter (unit)	Estimate	% RSE
k_{el} (h^{-1})	0.0382	48
V_c (L/kg)	0.0683	21
k_{cp} (h^{-1})	0.0806	11
k_{pc} (h^{-1})	0.0148	27
k_a (h^{-1})	0.0254	20
F	0.499	47
k_{int} (h^{-1})	0.173	29
ξ (fg/platelet)	0.0215	31
SC_{50} (ng/mL)	0.0520	16
K_D (ng/mL)	0.131	129
T_P (h)	142	5.1
T_{PLT} (h)	253	1.6
S_{max}	11.2	7.6
σ^2-PK	0.158	60
σ^2-PD	0.00851	24

N_P and T_{PLT}/N_{PLT}, respectively. The number of ten compartments was arbitrarily selected to get a smoothed distribution of cell lifespans. The precursor cells in the first age compartment P_1 were assumed to be produced at the zero-order rate, k_{in}, which is stimulated by romiplostim according to a Hill function as follows:

$$\frac{dP_1}{dt} = k_{in} \cdot \left(1 + \frac{S_{max} \cdot C}{SC_{50} + C}\right) - \frac{N_p}{T_p} \cdot P_1 \tag{10}$$

where C denotes the romiplostim-free serum concentration, S_{max} represents the maximal stimulation of the production rate of megakaryocytes, SC_{50} denotes the romiplostim-free serum concentration necessary to achieve a 50% level of the maximum production of megakaryocytes cell, and P_1 represents the amount of megakaryocyte cells in the first age compartment. Although romiplostim competes with eTPO for the same c-Mpl receptor and exerts the same pharmacological effect, eTPO concentrations were not incorporated into the PK-PD model because the endogenous levels were not consistently measured experimentally, and they were relatively low compared to the romiplostim serum concentrations achieved after drug administration and, consequently, the amount of eTPO bound to c-Mpl receptor is negligible relative to the amount of romiplostim bound to that receptor. The remaining N_P-1 precursor cell age-compartments can be expressed as follows:

$$\frac{dP_i}{dt} = \frac{N_p}{T_p} \cdot (P_{i-1} - P_i), \quad i = 2, \ldots, N_p \tag{11}$$

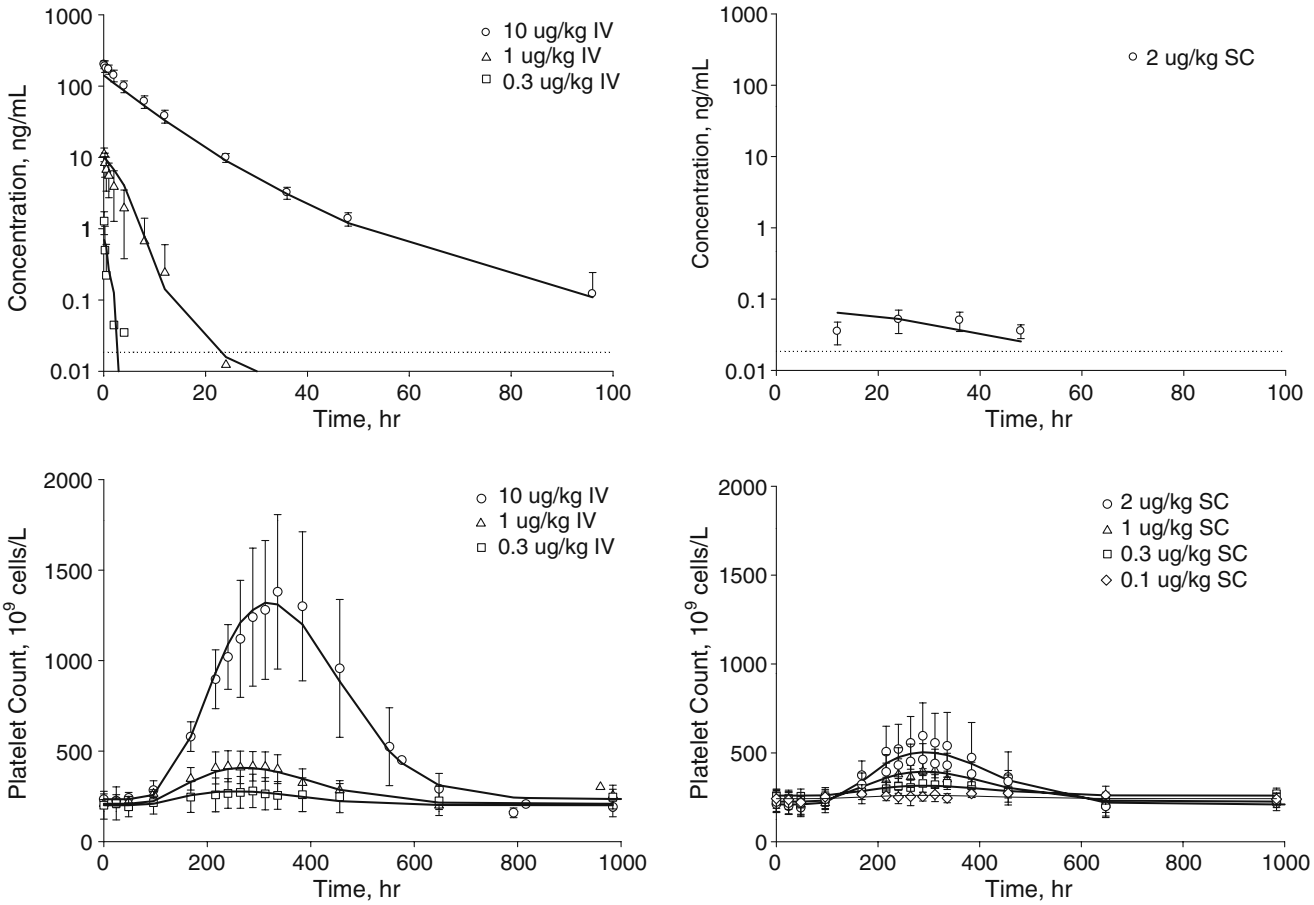

Fig. 2. Goodness-of-fit plots by the route of administration: pharmacokinetic data (*upper panel*), pharmacodynamic data (*lower panel*). The *symbols* represent the observed data with standard deviation represented in the *error bars* and the *lines* represent the model predictions. The lower limit of quantification for romiplostim ELISA assay was included as the *dashed line* in the pharmacokinetic profiles

The megakaryocytes generate the young platelets in the first age-compartment for platelets (PLT_1) according to Eq. 12:

$$\frac{dPLT_1}{dt} = \frac{N_P}{T_P} \cdot P_{N_P} - \frac{N_{PLT}}{T_{PLT}} \cdot PLT_1 \quad (12)$$

and platelets mature through a series of age-compartments as follows:

$$\frac{dPLT_j}{dt} = \frac{N_{PLT}}{T_{PLT}} \cdot (PLT_{j-1} - PLT_j), \quad j = 2, \ldots, N_{PLT} \quad (13)$$

Therefore, the number of circulating platelets is the sum of platelets at all ages according to Eq. 14:

$$PLT = PLT_1 + \ldots + PLT_{N_{PLT}} \quad (14)$$

As the only loss of cells from an age-compartment is into the next age-compartment, the random loss of cells was assumed to be negligible. Consequently, the lifespan parameters T_P and T_{PLT} become the apparent lifespan for the precursor cells and platelets, respectively. The initial conditions for P_i and PLT_j were determined from the baseline platelet count (PLT_0) as follows:

$$P_{i0} = \frac{T_P}{N_p \cdot T_{PLT}} \cdot PLT_0, \; i = 1, \ldots, N_P, \text{ and} \quad (15)$$

$$PLT_{j0} = \frac{PLT_0}{N_{PLT}}, j = 1, \ldots, N_{PLT} \quad (16)$$

The precursor cell production rate constant at baseline in Eq. 10 was calculated as follows:

$$k_{in} = \frac{PLT_0}{T_{PLT}} \quad (17)$$

This equation eliminated the necessity of including an amplifying factor between the last precursor compartment and first platelet compartment into the model, reflecting the fact that each megakaryocyte sheds approximately 4,000 platelets (16).

Statistical Model

Given the complexity of the model, population PK-PD analysis of the data in NONMEM failed. Inter-individual variability was not included in the statistical model because average data was used in the analysis. In addition, romiplostim serum concentrations below the limit of quantification were excluded in calculating the average data. The baseline platelet counts were fixed at the initial (predose) values for each dose level. The following error model was used to describe the residual variability:

$$Y_i = Y_{pred,i} \exp(\varepsilon_i) \quad (18)$$

where $Y_{pred,i}$ is the model-predicted value at time t_i, Y_i is the observed data, either C_i or PLT_i, and ε_i is an independent random variable that quantifies the deviations of the predicted data from the observed data. ε_i for the respective romiplostim serum concentration or platelet count data is assumed to follow a normal distribution with mean 0 and variance σ^2_{PK} or σ^2_{PD}, respectively.

Model Evaluation

Performance of the final PK-PD model was assessed via goodness-of-fit and simulations. PK and PD profiles were simulated over the dose range of 0.1–100 μg/kg for up to 200 and 1,200 h, respectively. The platelet response (ratio of the maximum platelet count to the baseline count) was generated from the simulated PD profiles. The simulated PK profiles were used to determine the area under the serum concentration-time curve (AUC). The dose (and AUC) *vs.* platelet-response curves were subsequently created based on the simulated data and were compared with the observed values. The model was considered acceptable if the simulated data fall within the 95% confidence interval of the mean observed data.

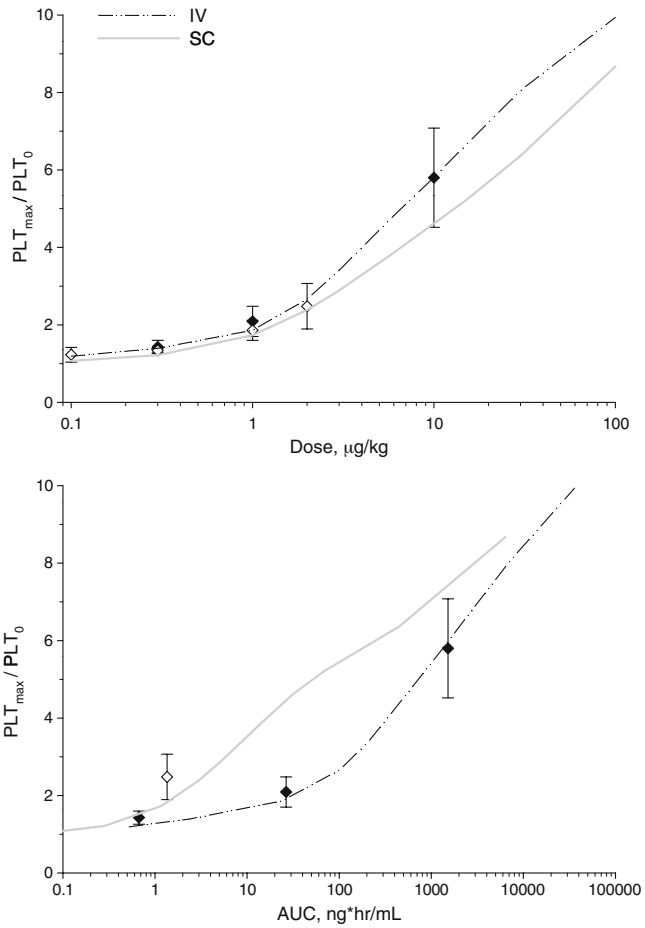

Fig. 3. Dose–response curves (*upper panel*) and AUC—response curves (*lower panel*). The *symbols* represent the observed values with standard deviation represented in the *error bars*, and *lines* represented simulated exposure–response curves using parameters presented in Table I

Model Application

Deterministic simulations were employed to explore the fraction of dose eliminated through the target-mediated pathway, to investigate the differences between the fractional receptor occupancy ($DR/R_{tot} = C/[K_D + C]$) and the fractional stimulatory effect ($C/[SC_{50} + C]$), and to better understand the role of the dose, the baseline platelet count, the administration route, and the dosing schedule (3 μg/kg weekly (QW), 6 μg/kg every 2 weeks (Q2W), and 9 μg/kg every 3 weeks (Q3W)) on the time course of romiplostim serum concentrations and the platelet counts.

RESULTS

Subjects

All subjects who were randomized completed this study. The participants in each cohort were demographically similar in terms of age, sex, race, and body weight (7). Only platelet data from romiplostim-treated subjects were included in the analysis as platelet counts did not change over time. The serum romiplostim concentrations for cohorts receiving IV doses and 2 μg/kg SC dose were used in the analysis as the serum concentration obtained after lower SC doses were below the limit of quantification. In total, 123 quantifiable serum concentrations in 17 participants and 481 platelet counts from 32 participants were included in this analysis.

PK-PD Model

Table I provides a summary of romiplostim PK-PD parameter estimates. The goodness-of-fit plots are displayed in Fig. 2 and show that the model characterized the PK data reasonably well. The estimate of the central volume of distribution indicated that romiplostim is primarily restricted to the blood compartment. Romiplostim is also distributed to the peripheral compartment, and the estimates of k_{cp} and k_{pc} were relatively precise. The estimate of K_D (0.131 ng/mL or 2.2 pM) was much lower than the literature-reported values for eTPO and recombinant human thrombopoietin (rHu-TPO) (10,17–19). The estimated k_{int} value was 0.173 h^{-1} indicating the internalization of romiplostim was the faster elimination process, and it was similar to the previously reported value for rHu-TPO (17).

For healthy subjects with platelet counts of 150-450×10^9 cells/L at baseline, the estimated total c-Mpl receptor concentration (ξ) of 0.022 fg/platelet (Table I) corresponds to approximately 50–150 pM and approximately 200 receptors/platelet cell). This is greater than an average of 56 TPO binding sites per platelet reported by Li *et al.* (8), suggesting that it reflects the total binding capacity of the thrombopoietic system for c-Mpl ligands, as reported for other TRAs (17, 20).

The PK-PD model characterized the PD data reasonably well (Fig. 2). Notably, the model captured the platelet count profiles even for the lowest SC doses where romiplostim serum concentrations were below the limit of quantification. The model contains two system-related parameters, T_P and

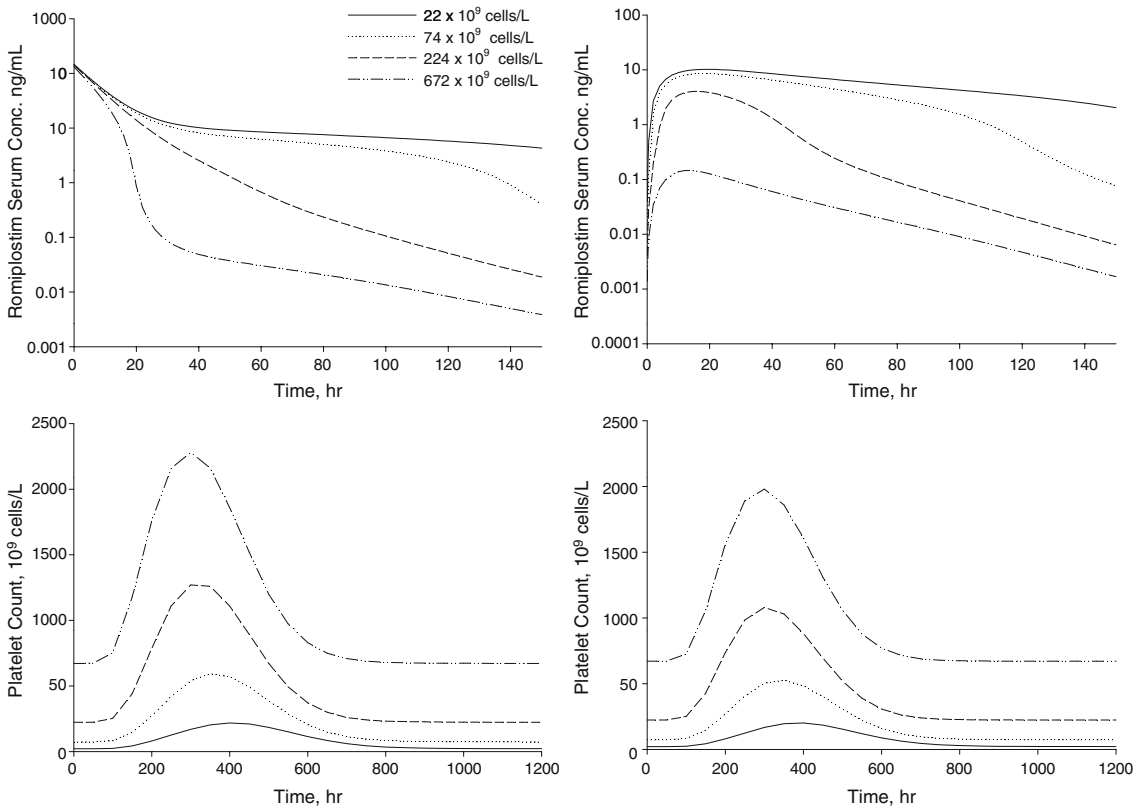

Fig. 4. Effect of platelet counts at baseline on romiplostim serum concentrations and platelet counts following administration of a single IV (*left panels*) or SC (*right panels*) dose of 10 μg/kg romiplostim

T_{PLT}, and two drug-dependent parameters, S_{max} and SC_{50}, which were all precisely estimated with RSE of 16% or lower (Table I). After romiplostim administration, platelet counts began to rise after a time delay, T_P, which was estimated to be 5.9 days (Table I) and is consistent with the reported megakaryocyte lifespan (7,21). The estimated value of platelet lifespan, $T_{PLT,}$ was 10.5 days, (Table I) and is in agreement with the literature range of 8–12 days (13). As previously demonstrated for lifespan models (22), the estimated time to peak platelet response (T_P+T_{PLT}) of 16.4 days is reflective of the sum of the megakaryocyte and platelet lifespans, which is similar to the observed time of maximum response of 10–14 days after dose (7). After the maximum platelet counts were achieved, they returned to the baseline 27 days after dose.

The predicted dose *vs*. platelet-response curves and exposure *vs*. platelet-response curves were within the 95% confidence interval of the mean observed data (Fig. 3), indicating the adequacy of the model to describe these relationships. Notably, the model-predicted maximum response ($1+S_{max}$, 12.2) was not reached at the highest dose studied.

Model Application

Baseline platelets counts play a significant role in the time course of romiplostim serum concentrations and platelet counts as illustrated in Fig. 4 for a single IV or SC dose of 10 μg/kg romiplostim in subjects with baseline platelet counts of 22, 74, 224, and 672×10^9 cell/L. The PK profiles with the highest romiplostim serum concentrations correspond to the lowest baseline platelet counts and *vice versa*. Interestingly, the platelet count profiles exhibit not only a shift due to the baseline difference but also an increase in the absolute change from the baseline and a reduction in the time to reach the maximum platelet count. In the order of increasing platelet baselines, the absolute increase in platelet counts for an IV dose was 196, 520, 1,046, and $1{,}608\times10^9$ cells/L, corresponding to relative changes of 891%, 703%, 467%, and 239%.

Figure 5 showed simulated time courses of the fraction of dose eliminated via receptor binding and internalization clearance following romiplostim IV and SC doses of 1, 3, and 10 μg/kg for baseline platelet counts of 10, 50, and 250×10^9 cells/L. At 250×10^9 cells/L, the linear clearance of romiplostim contributed minimally to the drug elimination as at least 90% of the SC dose administered was eliminated via the receptor-mediated clearances for all dose levels. With decreasing baseline platelet counts, the contribution of the receptor-mediated clearance decreased (e.g., 100%, 80%, and 40% for platelet baselines of 250, 50, and 10×10^9 cells/L, respectively, at 3 μg/kg IV dose) as the role of linear clearance becomes more prominent. The differences across three different

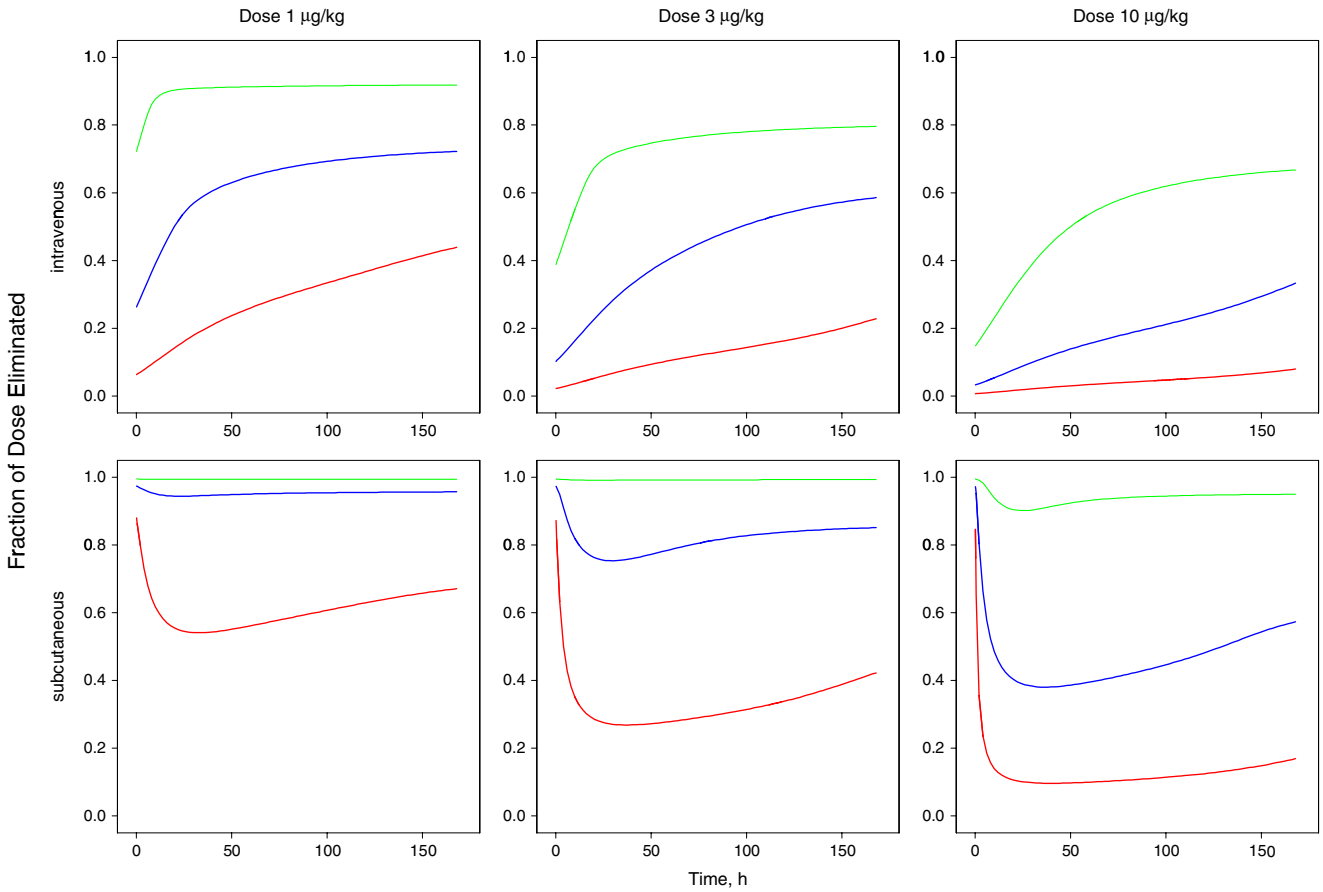

Fig. 5. Effect of dose and platelet counts at baseline on the fraction of dose eliminated via target-mediated clearance pathways *vs*. time following IV and SC dosing of romiplostim. Baseline platelet counts are 10×10^9 cells/L (*red line*), 50×10^9 cells/L (*blue line*), and 250×10^9 cells/L (*green line*)

baseline platelet counts were more evident for the SC route and they appeared to be dose dependent. Additionally after IV administration, the fraction of dose eliminated through the target-mediated pathway is consistently lower than that after the SC administration regardless of the baseline platelet count and dose level.

Simulated time course of the fraction of receptor occupancy and the fractional stimulatory effect are shown in Figs. 6 and 7, respectively, for IV and SC romiplostim dose of 1, 3, and 10 μg/kg and baseline platelets of 10, 50, and 250×10^9 cells/L. The maximum receptor occupancies for the normal baseline of 250×10^9 cells/L were approximately 100% immediately after the IV dose administration, and 15%, 40%, and 95% was achieved for increasing SC dose. The corresponding durations of at least 50% receptors occupied by romiplostim were about 10, 20, and 80 h for increasing IV doses whereas only the 10 μg/kg SC dose reached higher than 50% receptor occupancy and sustained over 60 h. As SC_{50} was lower than the K_D, the fraction of stimulatory effect was consistently higher than the fraction of receptor occupancy over 1 week period. A general relationship between the fraction of stimulatory effect (FS) and the fraction of receptor occupancy (FO) can be derived as follows:

$$FS = \frac{K_D \cdot FO}{SC_{50} + (K_D - SC_{50}) \cdot FO} \quad (19)$$

This relationship is independent of the dose, the route of administration, and the baseline platelet count. The receptor occupancy required to elicit 50% of the fractional stimulatory effect was 28% (Fig. 8) and only 60% receptor occupancy was needed for 80% of the stimulatory response. These results support the spare receptor theory (23) as an explanation to the romiplostim mechanism of action. This pharmacological theory has been previously reported for other TRAs (20, 23, 24).

Platelet responses were similar after IV and SC administration in healthy subjects receiving the same dose level (1 μg/kg) although romiplostim exposure was markedly lower (or not measurable) after SC administration relative to that observed after IV administration (Fig. 2). This paradoxical phenomenon is consistent with the above mentioned spare receptor theory because the IV dose has considerably more wastage relative to the SC dose. Figure 5 shows that a larger fraction of drug was eliminated via the target-mediated pathway following SC dosing, while the fraction of drug eliminated via the target-mediated pathway following IV dosing did not reach 100%. The SC dose provides relatively low and sustained romiplostim serum concentrations that are adequate to continuously stimulate the c-Mpl receptor. These effects are implicitly taken into account in the romiplostim PK-PD model, where the drug effect is characterized according to an E_{max} model. As shown in Fig. 7, an IV dose of 10 μg/kg in subjects with baseline platelet counts between 10 and 50×10^9 cell/L results in an almost full saturation of the

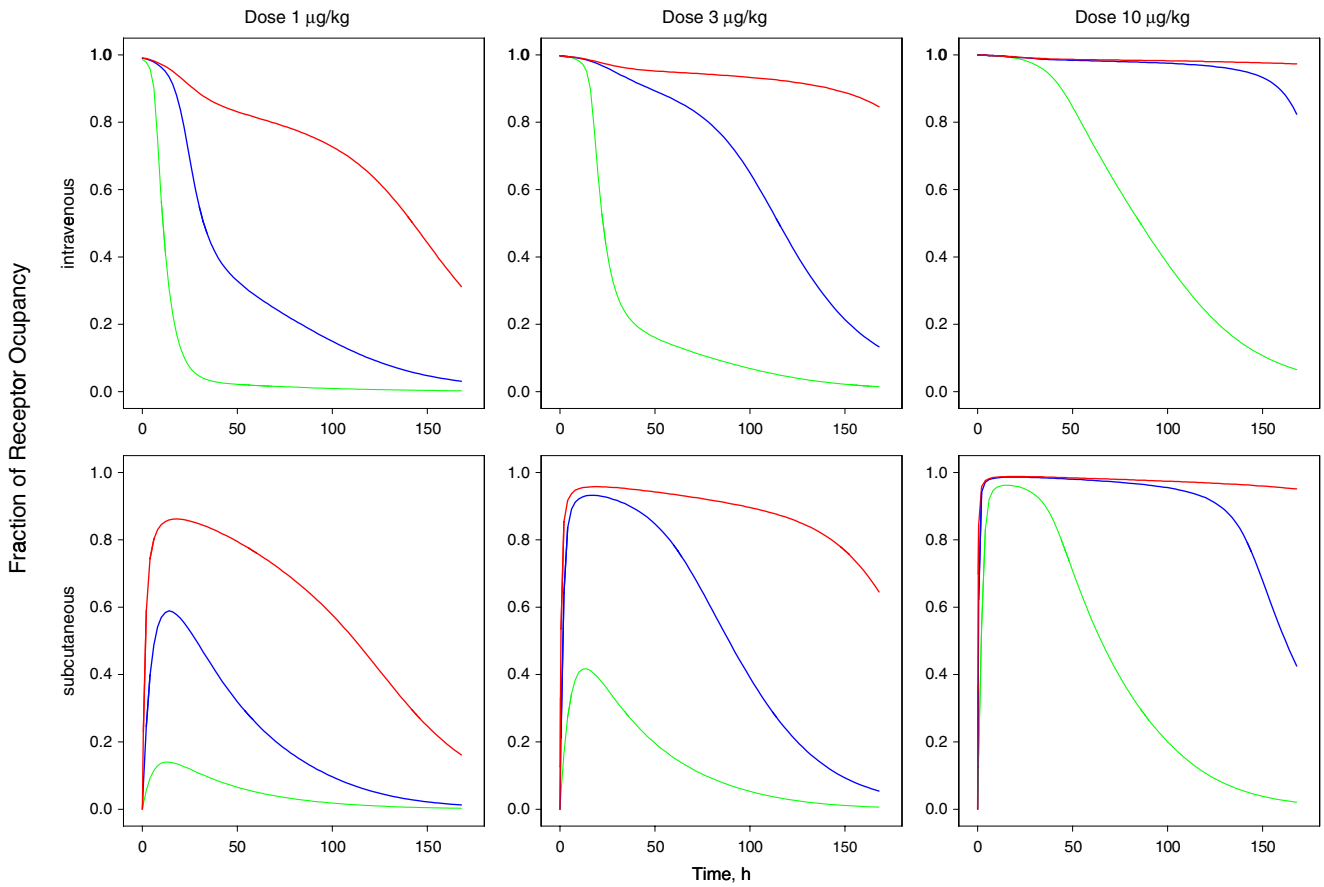

Fig. 6. Effect of dose and platelet counts at baseline on the time course of the typical fractional receptor occupancy following IV and SC dosing of romiplostim. Baseline platelet counts are 10×10^9 cells/L (*red line*), 50×10^9 cells/L (*blue line*), and 250×10^9 cells/L (*green line*)

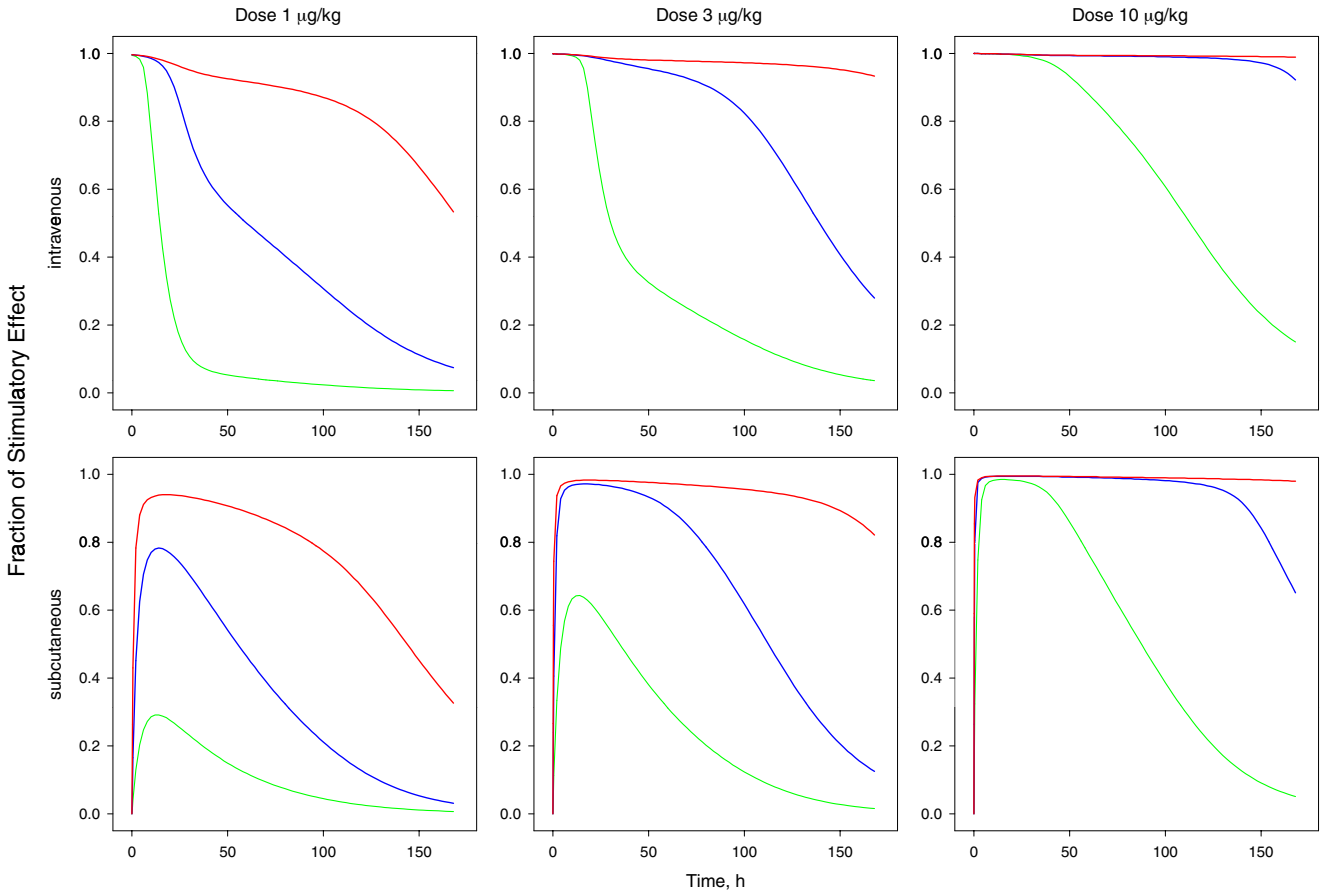

Fig. 7. Effect of dose and platelet counts at baseline on the time course of the typical fractional stimulatory effect following IV and SC dosing of romiplostim. Baseline platelet counts are ten (*red line*), 50 (*blue line*), and 250 (*green line*)$\times 10^9$ cells/L

stimulatory effect for 1-week period. As the dose decreases or the baseline platelet count increases, the profiles deviate earlier from the receptor saturation and, consequently, the stimulatory effect is maximized for a progressively shorter duration. This phenomenon is also observed following SC dosing.

Comparisons of simulated time course of typical romiplostim serum concentrations and platelet counts following 12-week repeated SC dosing of romiplostim in subjects with 10×10^9 cells/L baseline platelet count were presented in Fig. 9. Lower serum concentrations were observed after the second dose relative to the first dose for all regimens as a result of the increased platelet count after the first dose. Additionally, the simulations suggest that weekly dosing might maintain 50×10^9 cells/L platelet count with less fluctuation; probably because a weekly dosing interval is shorter than the sum of the megakaryocyte and platelet lifespans. The prolonged dosing intervals (Q2W and Q3W) are associated with increasing degrees of fluctuating platelet profiles over time, as the dosing interval was either similar to or greater than the sum of two lifespans.

DISCUSSION

The choice of a mechanistic PK-PD model should be based upon the known pharmacologic mechanisms of the system under investigation (25,26). The traditional PK-PD analysis usually involves a sequential approach whereby the PK model is developed first and then PK parameters are fixed to predicted drug concentrations, which are used as the driving functions in appropriate mechanism-based PK-PD models (17,27). The underlying assumption is that the amount of drug interacting with a pharmacological target or

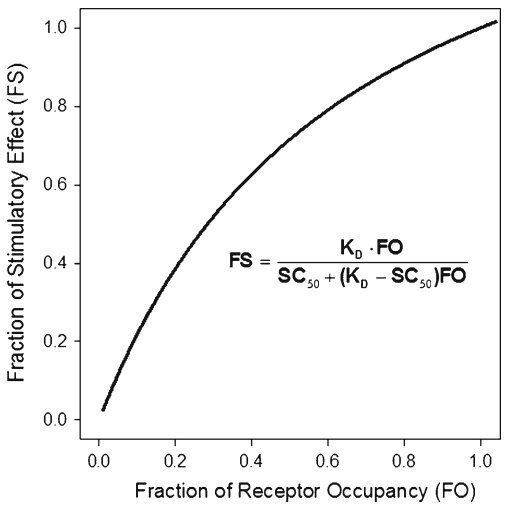

Fig. 8. A curve representing the relationship between the fraction of stimulatory effect (*FS*) and the fraction of the receptor occupancy (*FO*). This relationship is independent of the dose and route of administration

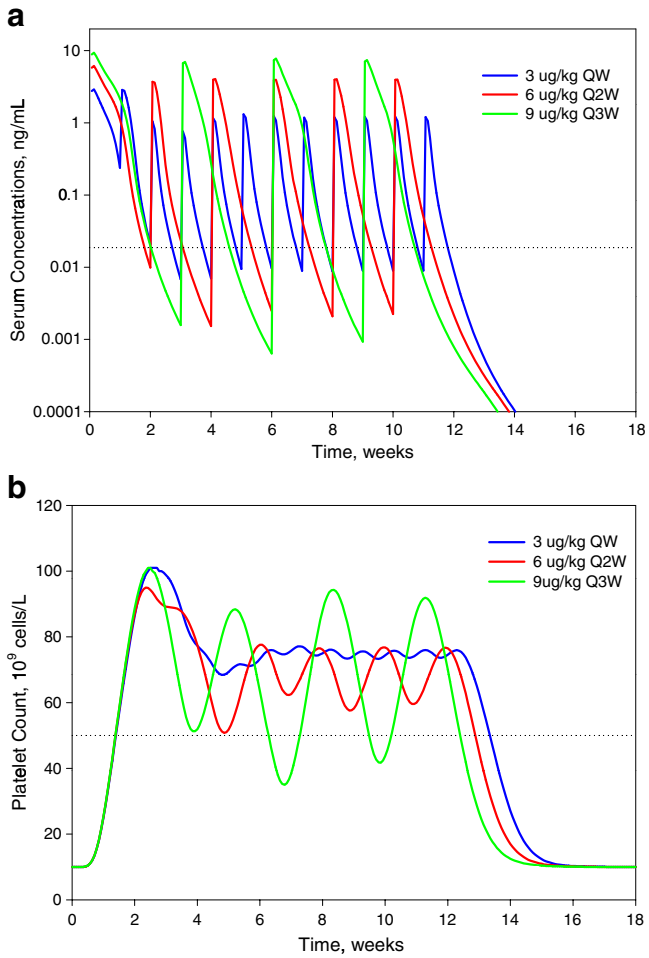

Fig. 9. Typical time course of romiplostim serum concentrations and platelet counts following repeated SC administration of 12 doses of 3 μg/kg QW, six doses of 6 μg/kg Q2W, and four doses of 9 μg/kg Q3W. The *dotted lines* represent the lower limit of quantification (18 pg/mL) of the bioanlaytical assay in the time course of serum concentration (*top panel*) and the platelet count of 50×10^9 cells/L in the time course of the platelet count (*bottom panel*)

distributing into a biophase is negligible relative to the overall dose and, consequently, the drug-receptor interaction does not alter the drug PK profile and the modelling of the PD data can be managed sequentially. This assumption is invalid for drugs exhibiting target-mediated disposition coupled with drug-mediated dynamic changes in the target amount as described by our PDMDD model which is a subtype of TMDD model. As in the case of romiplostim, a significant fraction of the drug, relative to the dose, is bound to the receptors (28) and the pharmacological action leads to a time-dependent change in the number of total receptors, which in turn results in a time-dependent PK. In this situation, the sequential approach is not applicable and simultaneous fitting of PK and PD data is more appropriate.

Romiplostim disposition involving endocytosis of drug-receptor complex was indicated by a dose-dependent decrease in clearance and the volume of distribution based on the non-compartmental analysis. Besides the effect of the drug-receptor interaction on the romiplostim serum concentration, the pharmacological response to romiplostim is also controlled by the drug-receptor interaction resulting in a dose-dependent increase in platelet counts, which in turn leads to an increased amount of receptors and a higher romiplostim clearance. This phenomenon represents a clear case where PD is influencing PK and, *vice versa* as evidenced in Fig. 9. Consistent with the principle of PDMDD model, platelet counts increased after romiplostim binding to the receptor which leads to a larger amount of free receptor available to clear romiplostim. Consequently, a lower baseline platelet count is associated with higher romiplostim serum concentrations and the PK profiles for low baseline platelet counts tend to show nonlinearity. This pharmacological understanding has been previously suggested (7) and informed the choice of the PK-PD model in Fig. 1. As both the exposure and the pharmacodynamic response of romiplostim are dependent on the dose administered as well as the baseline platelet counts, and the romiplostim PK is driven by the PD, it is of utmost importance to take into account a patient's platelet count during romiplostim therapy to individualize the dose to achieve the target response.

The complexity of the overall model with the differential equations involved prevented using the population approach and also created difficulties in performing nonlinear regression analysis even with mean data. The challenges notwithstanding, the model yielded parameter estimates that provided a reasonable characterization of the data and enabled simulations to test the appropriateness of the model for its intended use—understanding romiplostim pharmacology and exploring the exposure *vs.* platelet response after single and multiple doses administration to different target populations (29). Further efforts to characterize the population PK-PD model with new algorithms, such as SAEM, are ongoing.

The adequate characterization of the PK profiles was aided by the existence of adequate concentration-time data after IV doses. It is worth noting that romiplostim concentrations from SC administration were barely above limit of quantification for the highest dose tested, but the model adequately characterized the platelet-time course following the administration of SC doses. The imprecision in the K_D estimate is not unexpected given that accurate estimation of this parameter requires the implementation of very intensive PK sampling, in particular at concentration below the K_D. The region of drug concentrations lower than K_D is the most informative for the identifiability of the K_D parameter (30). However, it is also very close to the limit of quantification. Consequently, it is almost impracticable in the clinical setting to get a precise estimation of K_D in healthy subjects.

The estimate of K_D (2.2 pM) is much lower than the *in vitro* values reported for the eTPO for both platelets (100–200 pM) and megakaryocytes (749 pM), and was also slightly lower than the *in vivo* rHu-TPO K_D estimated using modeling techniques (45 pM) (10,17–19), which indicates that romiplostim has a high affinity for c-Mpl receptor.

While the presence of c-Mpl receptors on megakaryocytes was not explicitly accounted for in our model, the estimated ξ value corresponding to 200 c-Mpl receptors per platelet indicates this parameter value, mathematically, also accounts for the receptors on the precursor cells because it is greater than the reported value of 56 per platelet (8). Additionally, the nonzero estimate of ξ indicates the significance of receptor binding in romiplostim disposition.

The estimates of system-related parameters determine the shape of the time course of platelet counts and were consistent with previous literature (21). The delay in the time to peak platelet response and a prolonged duration of the PD effect with increasing dose of romiplostim, particularly for the profiles with low baseline platelet counts (Fig. 4), can be attributed to nonlinearity in PK. The PK nonlinearity resulted from saturation of the target-mediated clearance mechanism which leads to romiplostim serum concentrations being above the SC_{50} for a longer period of time. Its impact on PD is an increase in the time to achieve maximum platelet counts and to return to the baseline value.

From a pharmacological stand point, the 2.5-fold difference between SC_{50} and K_D values implies that a relatively low percentage of c-Mpl receptors need to be occupied in order to produce the pharmacodymamic effect. This suggests an indirect relationship between the binding to c-Mpl receptor and drug effect (19), consistent with the spare receptor theory (23) and the biochemical cascade in receptor signaling (1). We estimated a 28% receptor occupancy is needed to achieved 50% of the maximal stimulatory effect (Fig. 8), which is similar to the value previously reported by Samtani *et al.* (20). These results confirm the high potency of romiplostim and explain why platelet responses were similar after IV and SC administration receiving the same dose level, despite the large differences in the exposures.

Low doses of romiplostim given frequently is more efficient in achieving the target PD response than large doses given less frequently because the serum concentrations are sustained above the SC_{50} for a prolonged duration. Furthermore, repeated dosing at intervals shorter than the sum of the lifespans of megakaryocytes and platelets leads to sustained high platelets counts. In contrast, longer intervals lead to more fluctuation in the time course of platelets counts. In this context, weekly dosing will lead to smaller fluctuations in the platelet profile than Q2W and Q3W dosing (Fig. 9).

CONCLUSIONS

A model based on the principle of PDMDD as well as on the lifespan concepts was developed for romiplostim using a simultaneous PK-PD modeling approach. The choice of the PK model was based on the known pharmacologic mechanisms of the system under investigation. The model adequately described the observed PK and PD profiles and the exposure–response relationship. This approach provided not only a mechanistic explanation of platelet-dependent clearance of romiplostim but also allowed inference of some quantitative information about its pharmacology. The model can be a useful tool for the evaluation of dosing regimens targeting a particular platelet count or for the development of flexible dosing regimens.

A limitation of this model is that it uses data from healthy subjects after single-dose administration. It is anticipated that the appropriateness of the different dosing regimens will be defined using the intrinsic characteristics of the intended patient population, considering the disease effect on the lifespans of megakaryocytes and platelets and/or the potential effect of the concomitant medications as neither were accounted for within the single-dose study in healthy subjects.

ACKNOWLEDGMENTS

Part of the content of this manuscript was presented at a poster podium session at the 37th Annual Scientific Meeting of the International Society of Experimental Hematology and Society for Hematology and Stem Cells, Boston, USA, from 9 to 12 July 2008 (Wang YM, Pérez-Ruixo JJ, Xiao J, Jaramilla B, Chow A, Krzyzanski W. Pharmacokinetic and Pharmacodynamic Modeling of Romiplostim, a Novel Thromobopoietic Fc-Peptide Fusion Protein, in Healthy Subjects: a Semi-Mechanistic Approach).

The authors wish to thank Bing Wang and Dereck Amakye, principal investigator, for conducting the first time in man study for romiplostim, Bassam Abosaleem for coordinating the bioanalytical analysis for PK determinations, Bethlyn Jaramilla Sloey and Prerna Khandelwal for technical support and Ene Ette for the editorial comments provided during the preparation of the manuscript and Michelle Zakson for editing/writing assistance. The authors (Yow-Ming C Wang, Sameer Doshi, Jim Xiao, Juan Jose Perez-Ruixo, and Andrew T Chow) of this manuscript are employees of Amgen Inc. which supported this study. Wojciech Krzyzanski is a consultant for Amgen Inc. and received consultation fees for contributing to the current analysis.

REFERENCES

1. Geddis AE, Linden HM, Kaushansky K. Thrombopoietin: a pan-hematopoietic cytokine. Cytokine Growth Factor Rev. 2002;13:61–73.
2. Cardier JE, Dempsey J. Thrombopoietin and its receptor, c-mpl, are constitutively expressed by mouse liver endothelial cells: evidence of thrombopoietin as a growth factor for liver endothelial cells. Blood. 1998;91:923–9.
3. Sungaran R, Markovic B, Chong BH. Localization and regulation of thrombopoietin mRNa expression in human kidney, liver, bone marrow, and spleen using *in situ* hybridization. Blood. 1997;89:101–7.
4. Kuter DJ, Rosenberg RD. The reciprocal relationship of thrombopoietin (c-Mpl ligand) to changes in the platelet mass during busulfan-induced thrombocytopenia in the rabbit. Blood. 1995;85:2720–30.
5. Li J, Yang C, Xia Y, Bertino A, Glaspy J, Roberts M, *et al.* Thrombocytopenia caused by the development of antibodies to thrombopoietin. Blood. 2001;98:3241–8.
6. Basser RL, O'Flaherty E, Green M, Edmonds M, Nichol J, Menchaca DM, *et al.* Development of pancytopenia with neutralizing antibodies to thrombopoietin after multicycle chemotherapy supported by megakaryocyte growth and development factor. Blood. 2002;99:2599–602.
7. Wang B, Nichol JL, Sullivan JT. Pharmacodynamics and pharmacokinetics of AMG 531, a novel thrombopoietin receptor ligand. Clin Pharmacol Ther. 2004;76:628–38.
8. Li J, Xia Y, Kuter DJ. Interaction of thrombopoietin with the platelet c-mpl receptor in plasma: binding, internalization, stability and pharmacokinetics. Br J Haematol. 1999;106:345–56.
9. Fielder PJ, Hass P, Nagel M, Stefanich E, Widmer R, Bennett GL, *et al.* Human platelets as a model for the binding and degradation of thrombopoietin. Blood. 1997;89:2782–8.
10. Broudy VC, Lin NL, Sabath DF, Papayannopoulou T, Kaushansky K. Human platelets display high-affinity receptors for thrombopoietin. Blood. 1997;89:1896–904.
11. Mager DE, Jusko WJ. General pharmacokinetic model for drugs exhibiting target-mediated drug disposition. J Pharmacokinet Pharmacodyn. 2001;28:507–32.
12. Mager DE, Krzyzanski W. Quasi-equilibrium pharmacokinetic model for drugs exhibiting target-mediated drug disposition. Pharm Res. 2005;22:1589–96.

13. Harker LA, Roskos LK, Marzec UM, Carter RA, Cherry JK, Sundell B, *et al*. Effects of megakaryocyte growth and development factor on platelet production, platelet life span, and platelet function in healthy human volunteers. Blood. 2000;95:2514–22.
14. Roskos LK, Lum P, Lockbaum P, Schwab G, Yang BB. Pharmacokinetic/pharmacodynamic modeling of pegfilgrastim in healthy subjects. J Clin Pharmacol. 2006;46:747–57.
15. Perez-Ruixo JJ, Krzyzanski W, Hing J. Pharmacodynamic analysis of recombinant human erythropoietin effect on reticulocyte production rate and age distribution in healthy subjects. Clin Pharmacokinet. 2008;47:399–415.
16. Brown AS, Erusalamsky JD, Martin JF. Megakaryocytopoiesis: the megakaryocyte/platelet haemostatic axis. In: Franz von Bruchhausen UW, editor. Platelets and their factors. Berlin: Springer; 1997. p. 3–26.
17. Jin F, Krzyzanski W. Pharmacokinetic model of target-mediated disposition of thrombopoietin. Aaps J. 2004;6:86–93.
18. Sato T, Fuse A, Niimi H, Fielder PJ, Avraham H. Binding and regulation of thrombopoietin to human megakaryocytes. Br J Haematol. 1998;100:704–11.
19. Kuter DJ, Begley CG. Recombinant human thrombopoietin: basic biology and evaluation of clinical studies. Blood. 2002;100:3457–69.
20. Samtani MN, Perez-Ruixo JJ, Brown KH, Cerneus D, Molloy CJ. Pharmacokinetic and pharmacodynamic modeling of pegylated thrombopoietin mimetic peptide (PEG-TPOm) after single intravenous dose administration in healthy subjects. J Clin Pharmacol. 2009;49:336–50.
21. Jackson C, Arnold JT, Pestina TI, Stenberg PE. Megakaryocyte biology. In: Kuter DJ, Hunt P, Sheridan W, Zucker-Franklin D, editors. Thromobopoiesis and thrombopoietins; molecular, cellular, preclinical, and clinical biology. Totowa: Humana; 1997. p. 3–40.
22. Krzyzanski W, Ramakrishnan R, Jusko WJ. Basic pharmacodynamic models for agents that alter production of natural cells. J Pharmacokinet Biopharm. 1999;27:467–89.
23. Stephenson RP. A modification of receptor theory. Br J Pharmacol Chemother. 1956;11:379–93.
24. Holford N. Drug concentration, binding, and effect *in vivo*. Pharm Res. 1984;1:102–5.
25. Derendorf H, Meibohm B. Modeling of pharmacokinetic/pharmacodynamic (PK/PD) relationships: concepts and perspectives. Pharm Res. 1999;16:176–85.
26. Mager DE, Wyska E, Jusko WJ. Diversity of mechanism-based pharmacodynamic models. Drug Metab Dispos. 2003;31:510–8.
27. Zhang L, Beal SL, Sheiner LB. Simultaneous *vs.* sequential analysis for population PK/PD data I: best-case performance. J Pharmacokinet Pharmacodyn. 2003;30:387–404.
28. Levy G. Pharmacologic target-mediated drug disposition. Clin Pharmacol Ther. 1994;56:248–52.
29. Ette EI, Williams PJ, Kim YH, Lane JR, Liu MJ, Capparelli EV. Model appropriateness and population pharmacokinetic modeling. J Clin Pharmacol. 2003;43:610–23.
30. Abraham AK, Krzyzanski W, Mager DE. Partial derivative-based sensitivity analysis of models describing target-mediated drug disposition. Aaps J. 2007;9:E181–9.